ChemPubSoc Europe

DOI: 10.1002/cplu.201800139

CHEMPLUSCHEM Full Papers

Facile Synthesis of Palladium-Nanoparticle-Embedded N-Doped Carbon Fibers for Electrochemical Sensing

Kyubin Shim[+],[a] Zhong-Li Wang[+],*[b] Tasnima Haque Mou,[a] Yoshio Bando,[a, b] Abdulmohsen Ali Alshehri,[c] Jeonghun Kim,[d] Md. Shahriar A. Hossain,[a] Yusuke Yamauchi,*[d, e] and Jung Ho Kim*[a]

In recent years, there have been many studies on metal/carbon hybrid materials for electrochemical applications. However, reducing the metal content in catalysts is still a challenge. Here, a facile synthesis of palladium (Pd) nanoparticle-embedded N-doped carbon fibers (Pd/N-C) through electropolymerization and reduction methods is demonstrated. The as-prepared Pd/N-C contains only 1.5 wt% Pd. Under optimal conditions, bisphenol A is detected by using amperometry in two dynamic ranges from 0.1 to 10 μM and from 10 to 200 μM, and the obtained correlation coefficients are close to 0.9836 and 0.9987, respectively. The detection limit (DL) for bisphenol A is determined to be 29.44 (±0.77) nM.

Introduction

Noble metals have received much attention in many catalyst applications owing to their high catalytic activities.[1] Of these materials, platinum (Pt) is used in various applications because of its high activity, but it comes at a high cost. Many researchers have been studying various approaches to solving the cost problems by modifying materials to increase their surface area, the activity and selectivity of active sites, and their stability.[2] In particular, the shape- and size-controlled synthesis of noble-metal nanomaterials has received increasing attention because of their stimulation of catalytic reactions. Another modification method is to change the material. Palladium (Pd) can be used instead of platinum because its catalytic activity can be improved by modifying the material. In addition, Pd-based materials are about five times cheaper than Pt-based materials.[3]

Palladium nanoparticles are used widely in applications such as fuel cells, the oxidation of formic acid, and gas sensors.[4] The materials are modified by various methods, and the catalytic activity is highly dependent on the size and morphology of the Pd nanostructures.[4,5] These play a critical role in the performance over a wide range of applications. Pd nanoparticles that are used for composites enhance unique catalytic properties. Therefore, metal/carbon hybrid catalysts such as Pt/C and Pd/C are of great interest in terms of both increasing catalytic activity as well as decreasing the cost.[6]

There are diverse reports showing the enhanced electrocatalytic performances of metal/carbon hybrid materials, such as in sensors,[7,8] fuel cells,[9,10] and energy storage.[11,12] These catalysts are synthesized by depositing metal nanoparticles (NPs) onto the outer surface, inner surface, or interface of the support. The shapes of the metal nanoparticles or support materials influence their catalytic activity. In addition, a decrease in size of the metallic catalyst and an increased active area of the support materials improve their performance. As the catalyst active part of the support materials is increased, maintaining and/or improving performance, the amount of material used decreases. Metal/carbon hybrid materials such as metal/GO,[13,14] metal/SWCNT,[12,15] metal/MWCNT,[16,17] and metal/CNFs[18,19] have already been developed.

These materials have been used for the detection of various species. Among them, the detection of bisphenol A (2,2-bis(4-hydroxyphenyl) propane) is highly important, because bisphenol A can lead to health problems such as breast cancer, prostate cancer, birth defects, infertility, precocious development in girls, diabetes, and obesity.[20] Bisphenol A is one of the raw materials used to produce plastics and resins, and can be used for food containers, drink packaging, and to coat metal products (e.g., food cans, bottle tops).[21,22] Various methods have

[a] K. Shim,[+] T. H. Mou, Prof. Y. Bando, Dr. M. S. A. Hossain, Prof. J. H. Kim
Australian Institute of Innovative Materials (AIIM)
University of Wollongong
North Wollongong, NSW 2500 (Australia)
E-mail: jhk@uow.edu.au

[b] Dr. Z.-L. Wang,[+] Prof. Y. Bando
International Center for Materials Nanoarchitectonics (WPI-MANA)
National Institute for Materials Science (NIMS)
1-1 Namiki, Tsukuba, Ibaraki 305-0044 (Japan)
E-mail: Wang.Zhongli@nims.go.jp

[c] Prof. A. A. Alshehri
Department of Chemistry, King Abdulaziz University
P.O. Box. 80203, Jeddah 21589 (Saudi Arabia)

[d] Dr. J. Kim, Prof. Y. Yamauchi
School of Chemical Engineering &
Australian Institute for Bioengineering and Nanotechnology (AIBN)
University of Queensland, Brisbane, QLD 4072 (Australia)
E-mail: y.yamauchi@uq.edu.au

[e] Prof. Y. Yamauchi
Department of Plant & Environmental New Resources
Kyung Hee University, 1732 Deogyeong-daero, Giheunggu, Yongin-si
Gyeonggi-do 446-701 (South Korea)

[+] These authors contributed equally to this work.

Supporting information and the ORCID identification number(s) for the author(s) of this article can be found under: https://doi.org/10.1002/cplu.201800139.

been used for the detection of bisphenol A such as separation analysis,[23] fluorimetry,[24] immunoassay,[25] and electrochemical methods.[26] Of these, the electrochemical method has more advantages than other methods, such as short analysis time, simplicity, and great sensitivity. Because of this, electrochemical sensors using the direct oxidation reaction have been developed to detect bisphenol A, and this method requires electrochemically active electrode materials. The development of electrode materials is most important for good sensitivity.

Herein, we have focused on reducing the amount of Pd and successfully synthesized Pd-nanoparticle-embedded N-doped carbon fibers (Pd/N-C) with a Pd content of 1.5 wt%. The Pd/N-C hybrid material contains a small amount of Pd compared with other commercial Pd/C materials. Scanning electron microscopy (SEM), transmission electron microscopy (TEM), X-ray diffraction (XRD), and Raman spectroscopy were employed to characterize the Pd/N-C hybrid materials. Finally, we studied the application of the materials in the detection of bisphenol A.

Results and Discussion

The obtained Pd/N-C hybrid materials were obtained by electropolymerization and reduction methods (Figure 1a). The strategy for the synthesis of Pd/N-C hybrid materials can be summarized into four simple steps. First, the polyaniline (PANI) fibers were prepared by electrochemical polymerization in acid aniline solution. They were deposited on carbon paper and then stripped and dispersed in water. After washing three times, freeze-drying technology was used to remove the water to prevent the aggregation of the PANI fibers. By optimizing the type of acid, unique needle-branched nanostructures of PANI fibers were formed in HNO_3 electrolyte. Secondly, the polymer precursor was carbonized in nitrogen at 800 °C for 3 h, and was thus converted into N-doped carbon fibers. Thirdly, the resulting carbon fibers were soaked in water by ultrasonic dispersion, and then the quantitative Na_2PdCl_4 solution was added dropwise with stirring. Finally, the sample was dispersed in ethanol and reduced in a hydrogen atmosphere at 30 °C for 12 h.

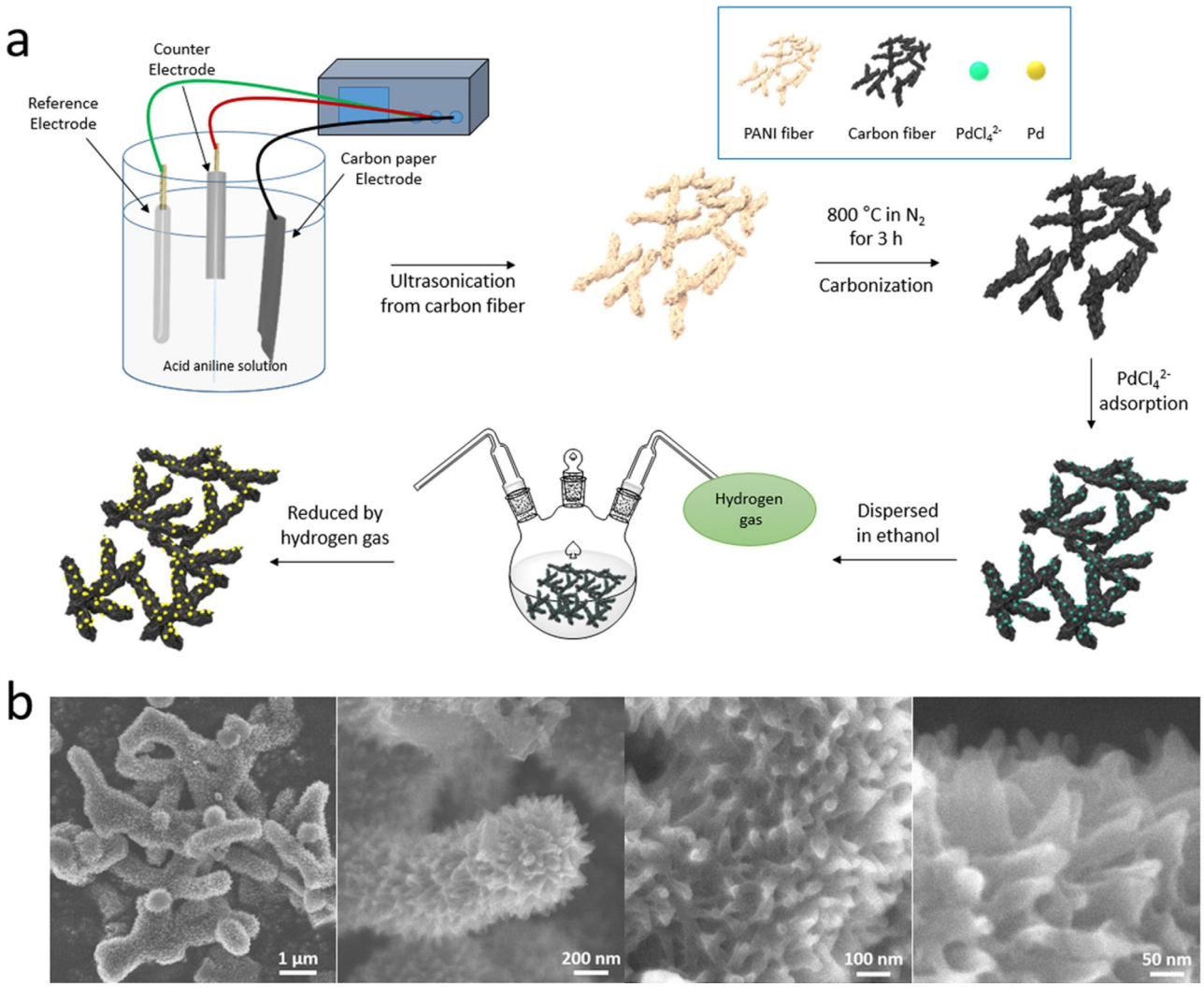

Figure 1. a) Schematic illustration of the synthesis of Pd/N-C hybrid material and b) SEM images of Pd/N-C hybrid material.

The obtained Pd/N-C hybrid materials and commercial Pd/C particles were confirmed by SEM (Figure 1b and Figure S1 in the Supporting Information). From these images, it can be confirmed that the Pd/N-C hybrid materials have a greater surface area than commercial Pd/C materials because of the specific shape of the Pd/N-C hybrid materials. Similarly to the shape identified in the SEM images, the unique nanostructural surface on the fibers was also confirmed by TEM observation (Figure 2a,b). For confirmation of the presence of Pd nanoparticles

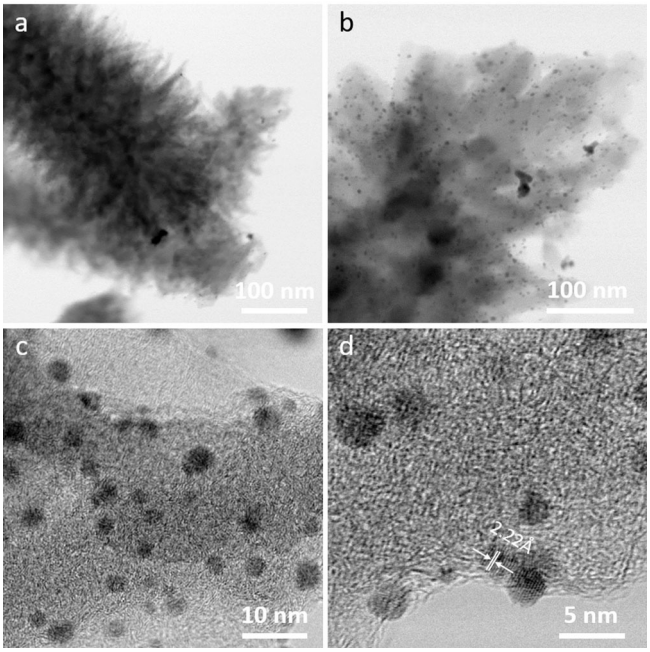

Figure 2. TEM images of Pd/N-C hybrid material: a,b) low magnification, and c,d) high magnification.

on the Pd/N-C fibers, the particles were observed directly by TEM. It was revealed that small Pd nanoparticles are formed on the carbon fibers and are evenly distributed (Figure 2c,d). The Pd content was determined to be 1.5 wt% by ICP measurement. Note that the Pd content can be tuned from low to high values by varying the reactant ratios. However, for a high content (>1.5 wt%), the size of the Pd nanoparticles will increase. By optimizing the electrochemical performances, it was found that the content of 1.5 wt% is the best value with the highest utilization efficiency of Pd. As seen in the Raman spectra of the Pd/N-C hybrid material, two peaks at 1598 cm^{-1} (G band) and 1320 cm^{-1} (D band) are observed (Figure S2), indicating a well-developed carbon matrix. The surface area was calculated to be 31 $m^2 g^{-1}$ by using the BET method and the obtained adsorption isotherm (Figure S3).

A high-resolution TEM image shows that the size of the Pd nanoparticles is around 3 nm. The nanoparticles show lattice fringes of around 0.22 nm, which is consistent with the d-spacing for the Pd (111) plane (Figure 2d). These images provided direct evidence that the Pd nanoparticles are well-crystalline and faceted. The wide-angle XRD peaks record the crystalline phase of the Pd/N-C hybrid material (Figure S4). The peaks of the Pd nanoparticles can be assigned to (111), (200), (220), and (311) diffraction peaks of the face-centered cubic (*fcc*) crystal structure. For further understanding of the Pd/N-C hybrid materials, HAADF-STEM images and elemental mapping were used, as shown in Figure 3. The Pd/N-C hybrid materials are

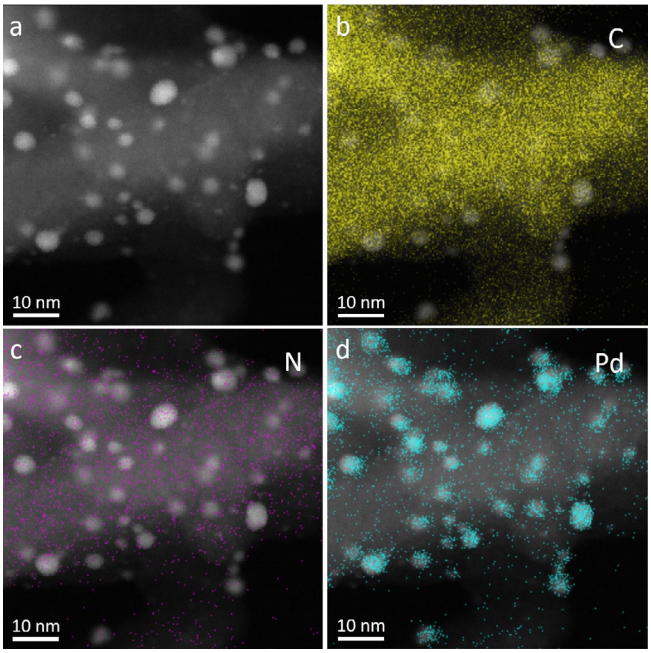

Figure 3. a) HAADF-STEM image, and b–d) elemental mapping images of Pd/N-C hybrid material.

composed of C, N, and Pd elements (Figure 3b–d). It is indicated that N and Pd are present on the carbon nanofiber. As seen in Figure 3d, Pd nanoparticles are clearly and uniformly distributed on the N-doped carbon fiber. In general, porous carbons are well known as catalytic support materials. Among them, N-doped porous carbon is one of the most interesting materials owing to properties such as enhanced catalytic activity, higher conductivity, and much higher resistance for coarsening.[26] Therefore, it is expected that Pd/N-C hybrid materials will improve the sensitivity for the detection of bisphenol A despite the lower amount of Pd.

Detailed XPS spectra were obtained to understand the chemical element states of the Pd/N-C hybrid material further. The survey results clearly show the presence of Pd 3d, C 1s, N 1s, and O 1s from the materials (Figure S5a). The contents of N, Pd, and C are 5.3, 1.2, and 93.5 wt%, respectively. Although several N-doped carbons by different approaches have been reported,[27–31] the N-doping is very effective for improving the electrical conductivity. Figure S5b–d (in the Supporting Information) reveals the high-resolution C 1s, N 1s, and Pd 3d spectra of the Pd/N-C material. As seen in Figure S5b, the high-resolution C 1s spectrum displays C–C, C–N, C–O, and C=O peaks, located at 284.8, 285.5, 286.5, and 288.8 eV, respectively. The deconvoluted N 1s peak of the Pd/N-C material reveals pyridinic N, pyrrolic N, and oxidized N located at 398.20, 400.40, and 402.90 eV, respectively (Figure S5c). The high-resolution Pd 3d

spectrum shows peaks appearing at 335.60 and 340.80 eV (Pd^0), and at 337.30 and 342.30 eV (Pd^{2+}) (Figure S5 d), indicating that the surface of the Pd nanoparticles is slightly oxidized.

The as-prepared electrode using the Pd/N-C hybrid material was tested for the electrochemical detection of bisphenol A. To realize the best performance, we checked the effect of the loading amount of the sample on the electrode. The Pd/N-C hybrid material suspension (3 μL, 1 mg mL^{-1}) was dropped on the electrode from one to four times. Then, cyclic voltammograms (CVs) were recorded using the electrodes modified with different amounts of the Pd/N-C hybrid materials (3–12 μL). The results revealed that 9 μL (three drops) was optimal (Figure S6). The Pd/N-C hybrid material and commercial Pd/C electrodes were activated by scanning the potential from 0.0 to 0.6 V at a scan rate of 0.1 V s^{-1} for ten cycles using cyclic voltammetry (CV). After activation, CVs were recorded in 5 to 100 μM by scanning the potential from 0.0 to 0.6 V at a scan rate of 0.05 V s^{-1}. During the scanning, the oxidation peak appeared clearly at around +0.23 V versus Ag/AgCl (vs. sat. KCl) (Figure 4 a). The calibration plots showed that the sensitivity of the Pd/N-C hybrid material electrode (slope = 0.0237 μA μM^{-1}) (black) is similar to that of the commercial Pd/C modified electrode (slope = 0.0228 μA μM^{-1}) (red) (Figure 4 b). Thus, we achieved a very high efficiency using the Pd/N-C hybrid material with only 1.5 wt% Pd. This efficiency is almost the same as that of the commercial material with a much higher Pd content (10 wt% Pd), which clearly has economic implications.

Chronoamperometric (CA) response curves were obtained with successive addition of different concentrations of bisphenol A in a 0.1 M PBS solution (Figure 4 c). To attain the maximum response current for BPA using the Pd/N-C hybrid modified electrode, the experimental conditions were optimized in terms of the starting and final applied potentials (Figure S7). In this case, the optimized starting and final applied potentials were determined to be +0.05 and +0.45 V, respectively. Two dynamic ranges of the calibration plot for bisphenol A detection were determined from 0.1 to 10 μM and from 10 to 200 μM, with correlation coefficients of 0.9836 and 0.9987, respectively (Figure 4 d). The two different linear ranges are caused by the different kinetics at different concentrations of bisphenol A. The oxidation kinetics in the low-concentration range were dominated by the adsorption process, whereas the kinetics in the high-concentration range depended on the BPA diffusion and activation by the catalyst.[32] The detection limit

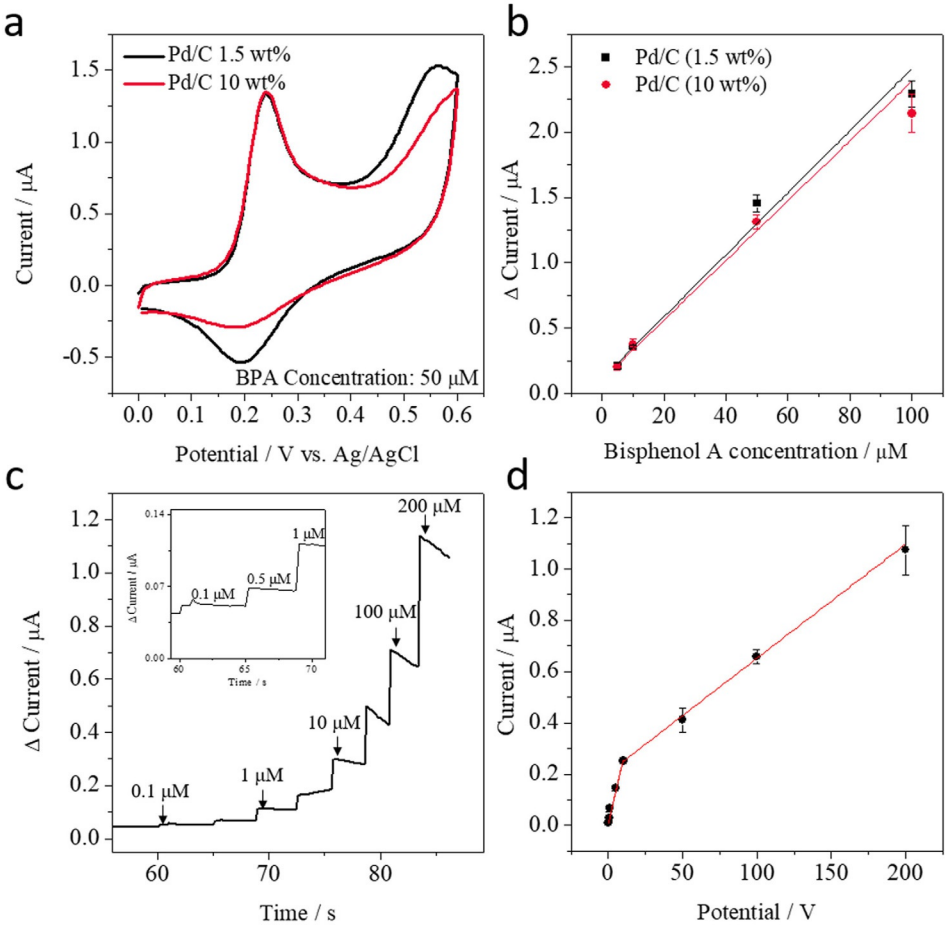

Figure 4. a,b) CVs for characterization of Pd/N-C hybrid material (with 1.5 wt% Pd) and Pd/C commercial material (10 wt% Pd): a) Detection of bisphenol A (50 μM) using Pd/N-C hybrid material and Pd/C commercial material electrodes. b) Bisphenol A detection (5, 10, 50, and 100 μM) calibration curves. c) Amperometric response of Pd/N-C hybrid material/AuNPs/SPCE with different concentrations of BPA. d) Calibration curves from the amperometric responses over two ranges of BPA concentration.

(DL) of bisphenol A was determined to be 29.44 (±0.77) nM. The threshold values of bisphenol A in water samples are already regulated by the European Chemicals Bureau. The values have defined predicted no-effect concentrations (PNEC) for fresh (1.5 μg L^{-1}) and marine (0.15 μg L^{-1}) waters.[33] Further comparison of our performance with previous literature is shown in Table S1 in the Supporting Information. Therefore, Pd/N-C hybrid materials can be used for electrode materials for the detection of bisphenol A.

Conclusion

We have successfully synthesized a Pd/N-C hybrid material by using electropolymerization and reduction methods. Small-sized Pd nanoparticles were loaded successfully on the carbon fibers. The Pd nanoparticles were distributed evenly on the carbon fibers without any aggregation. The Pd content was determined to be 1.5 wt% from ICP measurements. Interestingly, our Pd/N-C hybrid material shows very high efficiency, even though the loading amount of Pd is only 1.5 wt%, which is much lower than that of commercially available materials. The Pd/N-C hybrid modified electrode showed two dynamic ranges from 0.1 to 10 μM and from 10 to 200 μM, with a detection limit of 29.44 (±0.77) nM.

Experimental Section

Chemicals and materials

Aniline ($C_6H_5NH_2$, JIS Special Grade) and nitric acid (HNO_3, JIS Special Grade) were purchased from Wako Pure Chemical Industries, Ltd. Carbon paper (CP) was provided by Toray (Japan). Sodium tetrachloropalladate(II) (Na_2PdCl_4, 98.0%), monosodium phosphate (NaH_2PO_4), disodium phosphate (Na_2HPO_4), and bisphenol A were obtained from Sigma–Aldrich. Phosphate buffer solution (0.1 M, pH 7.4) was prepared by mixing solutions of 0.1 M NaH_2PO_4 and 0.1 M Na_2HPO_4.

Synthesis of Pd/*N*-C catalyst

PANI fibers were prepared through the galvanostatic method at a current density of 2 mA cm^{-2} for 2 h on a carbon paper (CP) electrode. Before use, the CP was treated at 500 °C in air for 1.5 h and washed with concentrated acid. The treated CP was used as the working electrode and the counter electrode, and a saturated calomel electrode (SCE) was used as the reference electrode. The electrolyte was prepared by dissolving HNO_3 (3.7 mL) in H_2O (44 mL), and then adding aniline (2.3 mL) to form a uniform solution. After electrochemical polymerization, PANI fibers were stripped from the CP and dispersed in water by ultrasonication. They were washed three times and freeze-dried for 24 h. The obtained polymer powder was then carbonized at 800 °C in a N_2 atmosphere for 3 h and converted into N-doped carbon. Next, the as-prepared carbon powder (40 mg) was dispersed in H_2O (40 mL) with ultrasonication for 2 h. Na_2PdCl_4 (1.67 mg) was dissolved in H_2O (40 mL). The Na_2PdCl_4 solution was then added dropwise to the carbon powder suspension. The sample was stirred for 2 h and washed three times, then dispersed in ethanol (20 mL) and transferred into a flask linked with a hydrogen balloon. The sample was reduced by hydrogen at 30 °C for 12 h with stirring. Then, the Pd/N-C catalyst was obtained after washing and vacuum drying.

Instruments

A screen-printed carbon electrode (SPCE) was used for the detection of bisphenol A. The area of the exposed working electrode that contained the carbon was 0.03141 cm^2. First, colloidal Au NPs in solution[34,35] were dropped onto the SPCE and dried. Secondly, the Pd/N-C hybrid (or commercial Pd/C) materials were dropped on the Au NP-modified SPCE and dried. The reference electrode was Ag/AgCl, and the counter electrode was pure carbon.[36,37] Amperograms and cyclic voltammograms (CVs) were recorded with a potentiostat/galvanostat (Ivium, Netherland). Microstructures were examined by TEM (JEOL ARM-200F, Japan) and SEM (JEOL JSM-7500). The surface area was calculated by the BET method using the obtained adsorption isotherm (BELSORP-mini II, MicrotracBEL Corp.). Wide-angle powder XRD patterns were measured with a GBC MMA XRD at a scanning rate of 2° min^{-1}. Raman spectroscopy was obtained with a JY HR800 instrument (HORIBA, Japan). XPS experiments were performed with a VG Scientific ESCALAB 2201XL instrument.

Acknowledgements

Z.W. thanks the Japan Society for Promotion of Science (JSPS) for providing the standard postdoctoral fellowship. This study was supported by an Australian Research Council (ARC) Future Fellow (FT150100479), the Suzuken Memorial Foundation, JSPS KAKENHI (grant numbers 17H05393 and 17K19044). This study was supported by the Deanship of Scientific Research (DSR), King Abdulaziz University, Jeddah, under grant number KEP-7-130-39.

Conflict of interest

The authors declare no conflict of interest.

Keywords: carbon · electrochemical sensing · electrochemistry · palladium · porous materials

[1] C. Zhu, D. Du, A. Eychmüller, Y. Lin, *Chem. Rev.* **2015**, *115*, 8896–8943.
[2] Y. Xia, X. Yang, *Acc. Chem. Res.* **2017**, *50*, 450–454.
[3] M. Shao, *J. Power Sources* **2011**, *196*, 2433–2444.
[4] A. Chen, C. Ostrom, *Chem. Rev.* **2015**, *115*, 11999–12044.
[5] H. Zhang, M. Jin, Y. Xiong, B. Lim, Y. Xia, *Acc. Chem. Res.* **2013**, *46*, 1783–1794.
[6] D. S. Su, S. Perathoner, G. Centi, *Chem. Rev.* **2013**, *113*, 5782–5816.
[7] V. R. Khalap, T. Sheps, A. A. Kane, P. G. Collins, *Nano Lett.* **2010**, *10*, 896–901.
[8] C. Rajkumar, P. Veerakumar, S.-M. Chen, B. Thirumalraj, S.-B. Liu, *Nanoscale* **2017**, *9*, 6486–6496.
[9] S. Chakraborty, C. R. Raj, *Carbon* **2010**, *48*, 3242–3249.
[10] H.-W. Liang, W. Wei, Z.-S. Wu, X. Feng, K. Müllen, *J. Am. Chem. Soc.* **2013**, *135*, 16002–16005.
[11] Y. Lei, J. Lu, X. Luo, T. Wu, P. Du, X. Zhang, Y. Ren, J. Wen, D. J. Miller, J. T. Miller, Y.-K. Sun, J. W. Elam, K. Amine, *Nano Lett.* **2013**, *13*, 4182–4189.
[12] V. R. Chitturi, M. Ara, W. Fawaz, K. Y. S. Ng, L. M. R. Arava, *ACS Catal.* **2016**, *6*, 7088–7097.
[13] M. Iqbal, C. Li, B. Jiang, M. S. A. Hossain, M. T. Islam, J. Henzie, Y. Yamauchi, *J. Mater. Chem. A* **2017**, *5*, 21249–21256.
[14] J.-J. Lv, S.-S. Li, A.-J. Wang, L.-P. Mei, J.-J. Feng, J.-R. Chen, Z. Chen, *J. Power Sources* **2014**, *269*, 104–110.

[15] J.-H. Lee, W.-S. Kang, C.-K. Najeeb, B.-S. Choi, S.-W. Choi, H.-J. Lee, S.-S. Lee, J.-H. Kim, *Sens. Actuators B* **2013**, *188*, 169 – 175.
[16] V. Bambagioni, C. Bianchini, A. Marchionni, J. Filippi, F. Vizza, J. Teddy, P. Serp, M. Zhiani, *J. Power Sources* **2009**, *190*, 241 – 251.
[17] H. An, H. Cui, D. Zhou, D. Tao, B. Li, J. Zhai, Q. Li, *Electrochim. Acta* **2013**, *92*, 176 – 182.
[18] G. Hu, F. Nitze, H. R. Brazegar, T. Sharifi, A. Mikolajczuk, C.-W. Tai, A. Borodzinski, T. Wågberg, *J. Power Sources* **2012**, *209*, 236 – 242.
[19] J. Huang, D. Wang, H. Hou, T. You, *Adv. Funct. Mater.* **2008**, *18*, 441 – 448.
[20] K. V. Ragavan, N. K. Rastogi, M. S. Thakur, *TrAC Trends Anal. Chem.* **2013**, *52*, 248 – 260.
[21] H. Yin, L. Cui, S. Ai, H. Fan, L. Zhu, *Electrochim. Acta* **2010**, *55*, 603 – 610.
[22] H. Yoshida, H. Harada, H. Nohta, M. Yamaguchi, *Anal. Chim. Acta* **2003**, *488*, 211 – 221.
[23] Z. Kuklenyik, J. Ekong, C. D. Cutchins, L. L. Needham, A. M. Calafat, *Anal. Chem.* **2003**, *75*, 6820 – 6825.
[24] X. Wang, H. Zeng, L. Zhao, J.-M. Lin, *Anal. Chim. Acta* **2006**, *556*, 313 – 318.
[25] M. A. Rahman, M. J. A. Shiddiky, J.-S. Park, Y.-B. Shim, *Biosens. Bioelectron.* **2007**, *22*, 2464 – 2470.
[26] X.-H. Li, M. Antonietti, *Chem. Soc. Rev.* **2013**, *42*, 6593 – 6604.
[27] Y. Chen, X. Li, K. Park, L. Zhou, H. Huang, Y.-W. Mai, J. B. Goodenough, *Angew. Chem. Int. Ed.* **2016**, *55*, 15831 – 15834; *Angew. Chem.* **2016**, *128*, 16063 – 16066.
[28] Y. Chen, J. Dong, L. Qiu, X. Li, Q. Li, H. Wang, S. Liang, H. Yao, H. Huang, H. Gao, J.-K. Kim, F. Ding, L. Zhou, *Chem* **2017**, *2*, 299 – 310.
[29] Y. Chen, X. Li, K. Park, W. Lu, C. Wang, W. Xue, F. Yang, J. Zhou, L. Suo, T. Lin, H. Huang, *Chem* **2017**, *3*, 152 – 163.
[30] R. R. Salunkhe, C. Young, J. Tang, T. Takei, Y. Ide, N. Kobayashi, Y. Yamauchi, *Chem. Commun.* **2016**, *52*, 4764 – 4767.
[31] R. R. Salunkhe, J. Tang, N. Kobayashi, J. Kim, Y. Ide, S. Tominaka, J. H. Kim, Y. Yamauchi, *Chem. Sci.* **2016**, *7*, 5704 – 5713.
[32] M. H. Naveen, N. G. Gurudatt, H.-B. Noh, Y.-B. Shim, *Adv. Funct. Mater.* **2016**, *26*, 1590 – 1601.
[33] G. M. Klečka, C. A. Staples, K. E. Clark, N. van der Hoeven, D. E. Thomas, S. G. Hentges, *Environ. Sci. Technol.* **2009**, *43*, 6145 – 6150.
[34] K. Shim, J. Kim, M. Shahabuddin, Y. Yamauchi, M. S. A. Hossain, J. H. Kim, *Sens. Actuators B* **2018**, *255*, 2800 – 2808.
[35] M. J. A. Shiddiky, Y.-B. Shim, *Anal. Chem.* **2007**, *79*, 3724 – 3733.
[36] N.-H. Kwon, K.-S. Lee, M.-S. Won, Y.-B. Shim, *Analyst* **2007**, *132*, 906 – 912.
[37] D.-M. Kim, S. J. Cho, C.-H. Cho, K. B. Kim, M.-Y. Kim, Y.-B. Shim, *Biosens. Bioelectron.* **2016**, *79*, 165 – 172.

Manuscript received: March 19, 2018